

Article

Mathematical Modeling of Water-Soluble Astaxanthin Release from Binary Polysaccharide/Gelatin Blend Matrices

Katarzyna Łupina ¹, Dariusz Kowalczyk ^{1,*} , Tomasz Skrzypek ² and Barbara Baraniak ¹

¹ Department of Biochemistry and Food Chemistry, Faculty of Food Sciences and Biotechnology, University of Life Sciences in Lublin, Skromna 8, 20-704 Lublin, Poland; katarzyna.lupina@gmail.com (K.Ł.); barbara.baraniak@up.lublin.pl (B.B.)

² Laboratory of Confocal and Electron Microscopy, Centre for Interdisciplinary Research, Faculty of Science and Health, John Paul II Catholic University of Lublin, Konstantynów 1J, 20-708 Lublin, Poland; tskrzypek@kul.lublin.pl

* Correspondence: dariusz.kowalczyk@up.lublin.pl

Abstract: Water-soluble AstaSana astaxanthin (AST) was loaded into 75/25 blend films made of polysaccharides (carboxymethyl cellulose (CMC), gum Arabic (GAR), starch sodium octenyl succinate (OSA), water-soluble soy polysaccharides (WSSP)) and gelatin (GEL) at levels of 0.25, 0.5, and 1%, respectively. Due to the presence of starch granules in the AST formulation, the supplemented films exhibited increased surface roughness as compared to the AST-free films. Apart from the CMC/GEL carrier, the migration of AST to water (25 °C, 32 h) was incomplete. Excluding the CMC-based carrier, the gradual rise in the AST concentration decreased the release rate. The Hopfenberg with time lag model provided the best fit for all release series data. Based on the quarter-release times ($t_{25\%}$), the 0.25% AST-supplemented OSA/GEL film ($t_{25\%} = 13.34$ h) ensured a 1.9, 2.2, and 148.2 slower release compared to the GAR-, WSSP- and CMC-based carriers, respectively. According to the Korsmeyer-Peppas model, the CMC-based films offered a quasi-Fickian release of AST ($n < 0.5$) with the burst effect ($t_{100\%} = 0.5\text{--}1$ h). In general, the release of AST from the other films was multi-mechanistic ($n > 0.5$), i.e., controlled at least by Fickian diffusion and the polymer relaxation (erosion) mechanism. The 1% AST-added WSSP/GEL system provided the most linear release profile.

Keywords: edible films; carboxymethyl cellulose; gum Arabic; octenyl succinic anhydride starch; water-soluble soy polysaccharides; gelatin; release rate; mathematical models; scanning electron microscopy



Citation: Łupina, K.; Kowalczyk, D.; Skrzypek, T.; Baraniak, B. Mathematical Modeling of Water-Soluble Astaxanthin Release from Binary Polysaccharide/Gelatin Blend Matrices. *Colloids Interfaces* **2021**, *5*, 41. <https://doi.org/10.3390/colloids5030041>

Academic Editor: Agnieszka Ewa Wiącek

Received: 18 June 2021

Accepted: 30 July 2021

Published: 3 August 2021

Publisher's Note: MDPI stays neutral with regard to jurisdictional claims in published maps and institutional affiliations.



Copyright: © 2021 by the authors. Licensee MDPI, Basel, Switzerland. This article is an open access article distributed under the terms and conditions of the Creative Commons Attribution (CC BY) license (<https://creativecommons.org/licenses/by/4.0/>).

1. Introduction

Hydrocolloids are commonly used in almost all major dosage forms including tablets, capsules, suspensions, gels, films, and transdermal patches [1]. Currently, plant origin polysaccharides, due to their abundance, renewability, and biodegradability, are often considered as an alternative material for packaging production, including “biodegr-edible” controlled-release packaging, which is a new technology that relies on releasing active compounds (antimicrobials and antioxidants) at desirable rates to extend the shelf life of food [2]. Edible packaging can be used where the application of plastic packaging is limited, e.g., as coating, casings, capsules, micro- and nano-capsules, sachets for single serve products (e.g., coffee, spices, etc.) that dissolve after exposure to heat, layers separating components in complex food, etc.

Every biopolymer has its own characteristic [3,4]. For example, the easily soluble polysaccharides, such as carboxymethyl cellulose (CMC) and pullulan, offer rapid release (burst effect) of bioactive molecules upon contact with the aqueous medium, while various forms of starch carrier matrices can be fabricated for controlled-release purposes [4,5]. The knowledge of release rate is of utmost relevance, hence a rapid release causes fast consumption of the active compounds within a short time, after which the concentration of active compound required for the effective protective action is not maintained on the food

surface; and, conversely, spoilage reactions on the food surface may start if the release of the preservatives from the packaging film is too slow [6].

To cover the shortcomings of some biopolymers, in order to obtain active packaging materials, which are capable of control preservative release for the whole storage period, the material properties are modified by blending, which is a simple and effective way to improve the performance of packaging biomaterials [7–9].

In general, gelatin (GEL), as a collagen derivative, forms more mechanically strong films compared to other biopolymers, such as cellulose derivatives, modified starches, gum Arabic (GAR), soy polysaccharides, and soy proteins [7,10]. The GEL films are poorly water-soluble at 25 °C [7], while dissolving immediately in biological fluids at body temperature [11]. Because of the excellent film-forming properties of GEL, many GEL-containing blend materials have been achieved, including the active edible packaging films [12–15]. The GEL-added polysaccharide films have less water-erodible character, thus exhibit slower release of food preservatives [16,17].

Astaxanthin (ASX) is one of the natural carotenoids present in *Haematococcus pluvialis*, yeast as well as in hydrobiontes, such as crab, shrimp, and salmon [18]. With its unique antioxidant power, and being superior to vitamin E, β -carotene, and coenzyme Q₁₀ [19], the ASX has attracted great attention in the scientific world. Nowadays, there are many publications describing the pro-healthy properties of ASX [20–22]. The technological improvements (e.g., micro-cultivation technologies with less water usage and electricity) in the production and commercialization of ASX has contributed to the market growth. Companies have employed cost-effective technologies to produce synthetic ASX. ASX from algae, synthetic and bacterial sources, is generally recognized as safe (GRAS) by the FDA [23]. Despite the fact that natural ASX has greater antioxidant capacity than the synthetic counterpart [24], the latter is about three times cheaper, more stable, oil-free, and water-soluble. Consequently, over 95% of the ASX available on the market is produced synthetically, whereas naturally produced microalgae ASX represents <1% of the commercial product [25]. On the basis of application, the global market for ASX is categorized into nutraceuticals, cosmetics, aquaculture, animal feed, and others.

Owing to its natural red color and capability of scavenging free radicals, ASX is the preferred choice for the active antioxidant packaging development [17,26] for specific applications, e.g., edible coatings for cheese, nuts, red meat, surimi sticks, etc.

In this work, the release of synthetic water-soluble AstaSana ASX (AST) from binary 75/25 blend films made of polysaccharides (carboxymethyl cellulose (CMC), GAR, starch sodium octenyl succinate (OSA), water-soluble soy polysaccharides (WSSP)) and gelatin (GEL) was determined at 25 °C (the highest predictable food/packaging contact temperature). The data were analysed mathematically by considering eight different release models. A comparative parametric study was performed to better understand the effects of AST concentration (0, 0.25, 0.5, 1%) along with carrier type on the release rate.

2. Materials and Methods

2.1. Materials

The food-grade biopolymers used in this study were: sodium CMC 30 GA (Dow Wolff Cellulosics, Bomlitz, Germany), GAR (Agri-Spray Acacia R, Agrigum International, Old Amersham, UK), starch sodium octenyl succinate Purity Gum 2000 (Ingredion Germany GmbH, Hamburg Germany), WSSP (Gushen Biological Technology Group Co. Ltd, Dezhou, China), and pork GEL (with bloom strength of 240; McCormick-Kamis S.A., Stefanowo, Poland). AstaSana 5% CWS/S-TG (containing astaxanthin, modified food starch, corn starch, glucose syrup, sodium ascorbate, and DL- α -tocopherol) was gifted by DSM Nutritional Products (Heerlen, The Netherlands). Glycerol and 2,2'-azino-bis(3-ethylbenzothiazoline-6-sulfonic acid) diammonium salt (ABTS) were purchased from Sigma Chemical Co. (Saint Louis, MO, USA).

2.2. Film Preparation

The films were prepared according to the previous procedure [17]. Briefly, the aqueous 5% (*w/w*) polysaccharide/GEL solutions containing glycerol (1% *w/w*) and AST (0.25, 0.5, 1% *w/w*) were degassed and cast on leveled polytetrafluoroethylene-coated trays with an area of 4 cm². The polysaccharide/GEL ratio was 75/25. A constant amount of total solids (0.0125 g/cm²) was placed on the trays in order to maintain film thickness. The film-forming solutions were dried at 25 ± 2 °C and 50 ± 5% relative humidity (RH) for 24 h. The films were peeled from the trays and conditioned in a MLR-350 climatic test chamber (Sanyo Electric Biomedical Co. Ltd., Osaka, Japan) for 48 h under the conditions as above.

2.3. Film Thickness

The thickness of the film samples (4 cm²) was determined using a 547–401 micrometer (Mitotuyo, Tokyo, Japan).

2.4. Scanning Electron Microscopy (SEM) and Light Microscopy

SEM was used in order to visualize the surface of the films, AST powder, and 1% AST aqueous solution. After drying in a Polaron CPD 7501 critical point dryer (Quorum Technologies Ltd., East Sussex, UK), the samples were sputter coated (Polaron SC7620, Quorum Technologies Ltd., East Sussex, UK) with 20–30 nm layer of gold palladium (Au/Pd) and examined using LEO 1430 VP scanning electron microscope (LEO Electron Microscopy Ltd., Cambridge, UK) at following presets: accelerating voltage of 15 kV, aperture size: 30 µm, beam current 30 µm, signal: secondary electron detector, chamber pressure: 10^{−5} Pa, working distance: 10–13 mm, image resolution: 2048 × 1576 pixel, scanning mode: pixel noise reduction. Additionally, the AST aqueous solution was examined with the Olympus MCKX53 light microscope (Olympus, Tokyo, Japan).

The diameter of the objects was measured using AxioVision Rel. 4.8 software (Carl Zeiss Microscopy GmbH, Göttingen, Germany).

2.5. AST Release Study

The film discs (4 cm²) were shaken with distilled water (25 mL, 25 ± 1 °C, 170 rpm, 32 h) in the shaking incubator (Incu-Shaker Mini, Benchmark Scientific, Inc., Sayreville, NJ, USA). 250 µL of the release media samples were taken at different time points and the absorbance was read at 464 nm using a microplate spectrophotometer (EPOCH 2 Microplate Spectrophotometer, BioTek, Winooski, VT, USA). The release tests were limited to 32 h because of a further progressive spoilage of film samples (the presence of a bad odour coming from the acceptor solution). The analyses were performed in triplicate.

2.6. Mathematical Modeling

DDSolver, i.e., add-in software for Microsoft Excel, was used for modeling the AST release kinetics. Eight mathematical models (Table 1) were chosen to fit the experimental data. The adjusted coefficient of determination (R^2_{adjusted}) was used for the selection of the optimal mathematical models, which were used for the determination of the quarter-release times ($t_{25\%}$) [27].

Table 1. Mathematical models used to describe the dissolution curves [27].

Model	Equation	Parameters
Zero-order with T_{lag} (Z-O T_{lag})	$F = k_0 \cdot (t - T_{lag})$	k_0, T_{lag}
First-order with F_{max} (F-O F_{max})	$F = F_{max} \cdot (1 - e^{-k_1 \cdot t})$	k_1, F_{max}
Higuchi with T_{lag} (Hig T_{lag})	$F = k_H \cdot (t - T_{lag})^{0.5}$	k_H, T_{lag}

Table 1. Cont.

Model	Equation	Parameters
Hopfenberg with T_{lag} (Hop T_{lag})	$F = 100 \cdot \left\{ 1 - \left[1 - k_{HB} \cdot (t - T_{lag}) \right]^n \right\}$	k_{HB}, n, T_{lag}
Korsmeyer–Peppas with T_{lag} (K-P T_{lag})	$F = k_{KP} \cdot (t - T_{lag})^n$	k_{KP}, n, T_{lag}
Logistic 2 (Log 2)	$F = F_{max} \frac{[e^{\alpha + \beta \cdot \log(t)}]}{1 + e^{\alpha + \beta \cdot \log(t)}}$	α, β, F_{max}
Makoid–Banakar with T_{lag} (M-B T_{lag})	$F = k_{MB} \cdot (t - T_{lag}) \cdot \text{Exp} \left[-k \cdot (t - T_{lag}) \right]$	k_{MB}, n, k, T_{lag}
Weibull with F_{max} (Wb F_{max})	$F = F_{max} \cdot \left[1 - e^{-\frac{(t-Ti)^\beta}{\alpha}} \right]$	$\alpha, \beta, Ti, F_{max}$

F is the fraction (%) of drug released in time t . k_0 is the zero-order release constant; k_1 is the first-order release constant; F_{max} is the maximum fraction of the drug released at infinite time; T_{lag} is the lag time prior to drug release. k_{HB} is the combined constant in Hopfenberg model, $k_{HB} = k_0 / (C_0 \times a_0)$, where k_0 is the erosion rate constant, C_0 is the initial concentration of drug in the matrix, and a_0 is the initial radius for a sphere or cylinder or the half thickness for a slab; n is 1, 2, and 3 for a slab, cylinder, and sphere, respectively; k_{KP} is the release constant incorporating structural and geometric characteristics of the drug-dosage form; n is the diffusional exponent indicating the drug release mechanism; α is the scale factor in Logistic 1 and 2 models; β is the shape factor in Logistic 1 and 2 models. k_{MB} , n , and k are empirical parameters in Makoid–Banakar model ($k_{MB}, n, k > 0$); α is the scale parameter which defines the time scale of the process; β is the shape parameter which characterizes the curve as either exponential ($\beta = 1$; case 1), sigmoid, S-shaped, with upward curvature followed by a turning point ($\beta > 1$; case 2), or parabolic, with a higher initial slope and after that consistent with the exponential ($\beta < 1$; case 3); Ti is the location parameter which represents the lag time before the onset of the dissolution or release process and in most cases will be near zero.

3. Results

3.1. Microstructure and Film Thickness

Consistent with the previous study [14], the surface of the control CMC/GEL film revealed the presence of GEL-rich microspheres with diameters ranging from 13.33 to 26.67 μm (Figure 1). It confirms that CMC and GEL are two incompatible biopolymers [8] that cannot form the homogeneous blend films at the micro-level. In turn, good compatibility (lack of aggregates or undissolved particles) was found for the other polysaccharide/GEL blends. In accordance with the previous studies [7], the surfaces of WSSP-containing film were rough and uneven, which could be attributed to the weak dissolution of the polysaccharide. The AST-added films were more heterogeneous as compared to the controls (Figure 1). Since starch is the component of the AST formulation (Figure 2), it is easy to deduce that the observed round-shaped inequalities were the starch granules. The size of the starch granules in the AST powder and the dehydrated AST solution ranged from 5.71 to 15.71 (Figure 2), which corresponds to the size of corn starch granules [28].

It was found that the CMC75/GEL25 films with higher AST content (0.5–1%) exhibited higher thickness as compared to other carriers ($p < 0.05$, Table 2). This result may be explained by the fact that the combination of the phase-separated microspheres with the starch granules (from AST) was unable to form a compact film network (Figure 1). However, regardless of the carrier type, no difference ($p > 0.05$) in thickness was observed between the AST-added and control films.

3.2. Release of AST

Figures 3 and 4 show the cumulative amount (mg/cm^2) and percentage of AST released from the films, respectively. It was found that during 32 h dissolution test, only the CMC/GEL carrier offered complete release. Depending on the AST concentration, the 100% release occurred after 0.5–1 h (Figure 4). This result could be easily explained by the fact that CMC dissolves rapidly after coming into contact with water [8]. The $t_{25\%}$ values estimated for the CMC-based films ranged from 0.09 to 0.15 h (Table 2). In the case of the other carriers, ~14–89% of the initial dose of AST was released. The slowest release of AST was found for the OSA/GEL ($t_{25\%} =$ from 13.34 to >27.26 h) and the WSSP/GEL ($t_{25\%} = 6.16$ – 50.95 h) carriers (Table 2). This result is likely associated with the partial solubility of these films at 25 °C [7]. It should be noted here that since the release of AST from the 1% AST-added OSA-based film was very slow and incomplete, it was not possible to predict $t_{25\%}$ for this system.

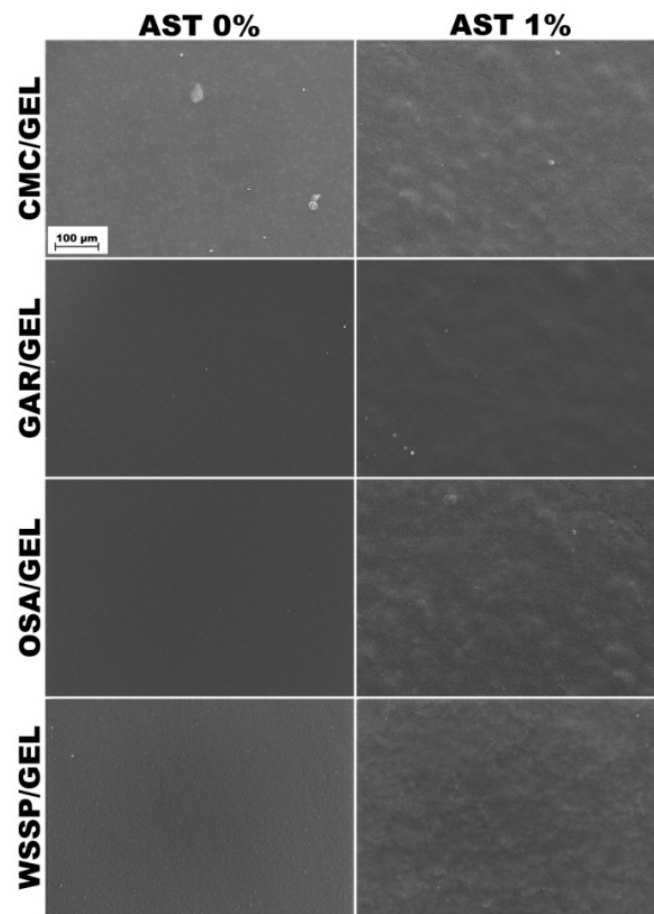


Figure 1. SEM images of the surfaces of the AST-free and 1%AST-added binary blend films based on polysaccharides (CMC, GAR, OSA and WSSP) and gelatin (GEL).

Table 2. Film thickness and the quarter-release times ($t_{25\%}$) obtained from the best fitting mathematical models.

Film	AST (%)	Thickness (μm)	$t_{25\%}$ (h)
CMC/GEL	0	91.32 ± 3.96 ^{ab}	-
	0.25	91.01 ± 3.23 ^{ab}	0.09 (<i>Wb Fmax</i>)
	0.5	95.88 ± 3.71 ^b	0.15 (<i>Wb Fmax</i>)
	1	94.17 ± 2.19 ^b	0.09 (<i>Wb Fmax</i>)
GAR/GEL	0	88.90 ± 2.40 ^a	-
	0.25	86.74 ± 3.21 ^a	7.20 (<i>M-B Tlag</i>)
	0.5	87.26 ± 3.87 ^a	22.27 (<i>M-B Tlag</i>)
	1	88.88 ± 2.33 ^a	24.00 (<i>M-B Tlag</i>)
OSA/GEL	0	88.33 ± 1.86 ^a	-
	0.25	86.39 ± 3.68 ^a	13.34 (<i>M-B Tlag</i>)
	0.5	87.72 ± 2.55 ^a	27.26 (<i>K-P Tlag</i>)
	1	86.67 ± 3.61 ^a	n.c. (<i>M-B Tlag</i>)
WSSP/GEL	0	88.88 ± 2.71 ^a	-
	0.25	88.21 ± 2.02 ^a	6.16 (<i>Log 2</i>)
	0.5	87.57 ± 3.73 ^a	17.46 (<i>Log 2</i>)
	1	86.75 ± 2.10 ^a	50.95 (<i>M-B Tlag</i>)

^{a,b} values with the different superscript letters are significantly different ($p < 0.05$); n.c.—not calculated; (*K-P Tlag*) Korsmeyer–Peppas with T_{lag} ; (*Log 2*) Logistic 2; (*M-B Tlag*) Makoid–Banakar with T_{lag} ; (*Wb Fmax*) Weibull with F_{max} .

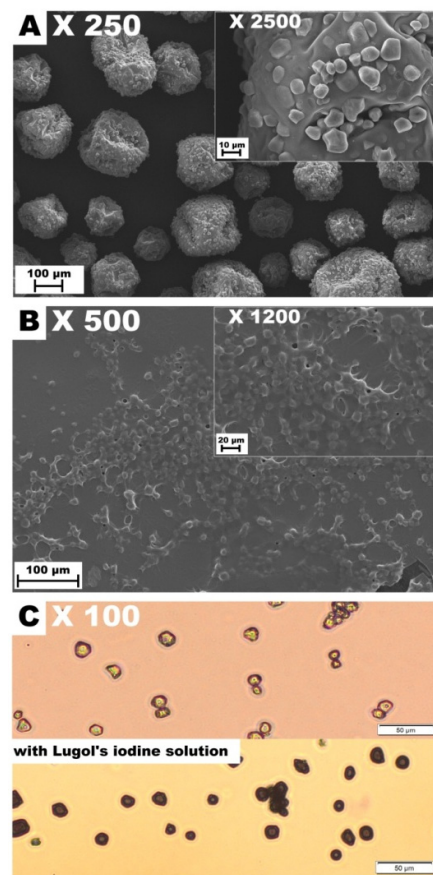


Figure 2. Images of AstaSana powder (A) and the dehydrated AstaSana aqueous solution examined using the scanning electron microscopy (B). The aqueous solution of AstaSana examined using the optical microscopy (C).

Regardless of the AST concentration, the WSSP/GEL film ensured the longest time without AST release ($T_{lag} = 50$ min, Figure 4). It suggests a strong physicochemical entrapment of the carotenoid in this matrix. This result confirms our earlier observations, which showed that WSSP-based film offered longer T_{lag} (thus slower release) than GAR-based carrier [17]. As suggested before, the cause could be the highly branched structure of WSSP [29]. Apart from the 1% AST-added WSSP-based system, the release profiles exhibited a sudden burst of AST. This phenomenon can be attributed to the erosion of the films.

Apart from the CMC-based carrier, the gradual rise in the AST concentration decreased the release rate from the carriers. It seems possible that this result is due to increasing amounts of the starch in the AST-added films; i.e., the starch granules (Figure 1) inhibited access of water molecules to the polymeric matrix, which limited dissolution of AST [17]. The highly erodible character of CMC probably meant that the presence of starch did not affect the dissolution behavior of the CMC/GEL carrier.

Eight mathematical equations (Table 1) were used to the quantitative interpretation of the data obtained from the ASTA release assay. The $R^2_{adjusted}$ and the parameter values estimated for the models are presented in Tables 3–6. It was impossible to fit one optimal model to describe the migration of AST from the particular carrier types, however, based on $R^2_{adjusted}$ averages the *Hop* T_{lag} model provided the best fit for all release series data ($R^2_{adjusted}$ mean = 0.9242). It was found that the *Hig* T_{lag} model was the least useful for AST release prediction ($R^2_{adjusted}$ mean = 0.6650). Among the tested models, the *F-O* F_{max} , *K-P* T_{lag} , *Hop* T_{lag} , *Log* 2, and *Wb* F_{max} were quite suitable for the description of AST release from the CMC-based carrier ($R^2_{adjusted} = 0.9410$ – 0.9890). The *Wb* F_{max} model ensured the

best fit ($R^2_{\text{adjusted}} = 0.9610\text{--}0.9890$). The shape parameter (β) obtained from the $Wb F_{\text{max}}$ model, showed that the AST release profile of the 0.25–0.5% AST-added CMC-based films was sigmoid ($\beta > 1$), while for the 1% AST-added carrier the release was more parabolic ($\beta < 1$). Nevertheless, the differences in the over mentioned shapes of the release curves were barely visible (Figures 4 and 5).

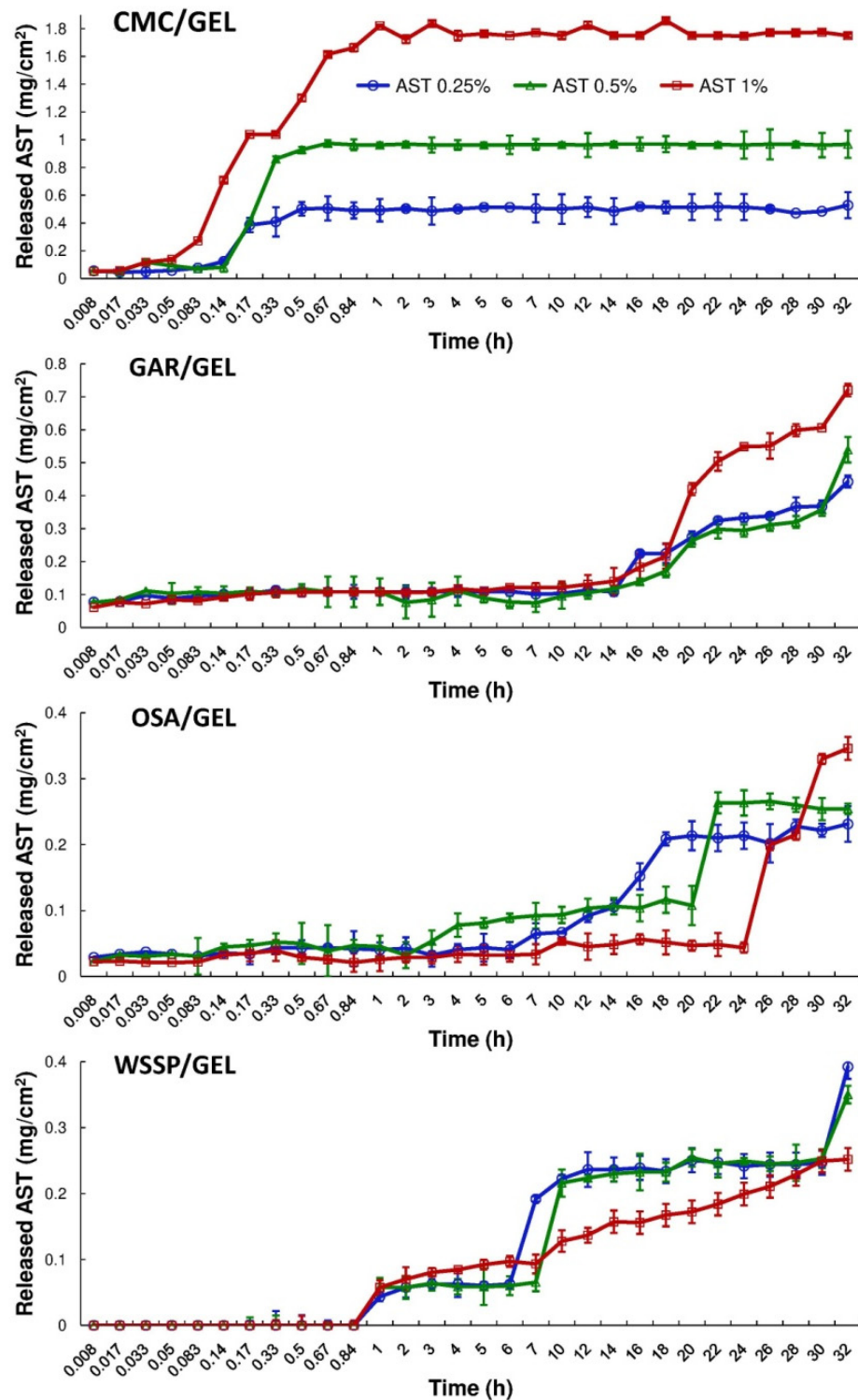


Figure 3. Cumulative migration of AST from the binary polysaccharide/GEL blend films into the water at 25 °C.

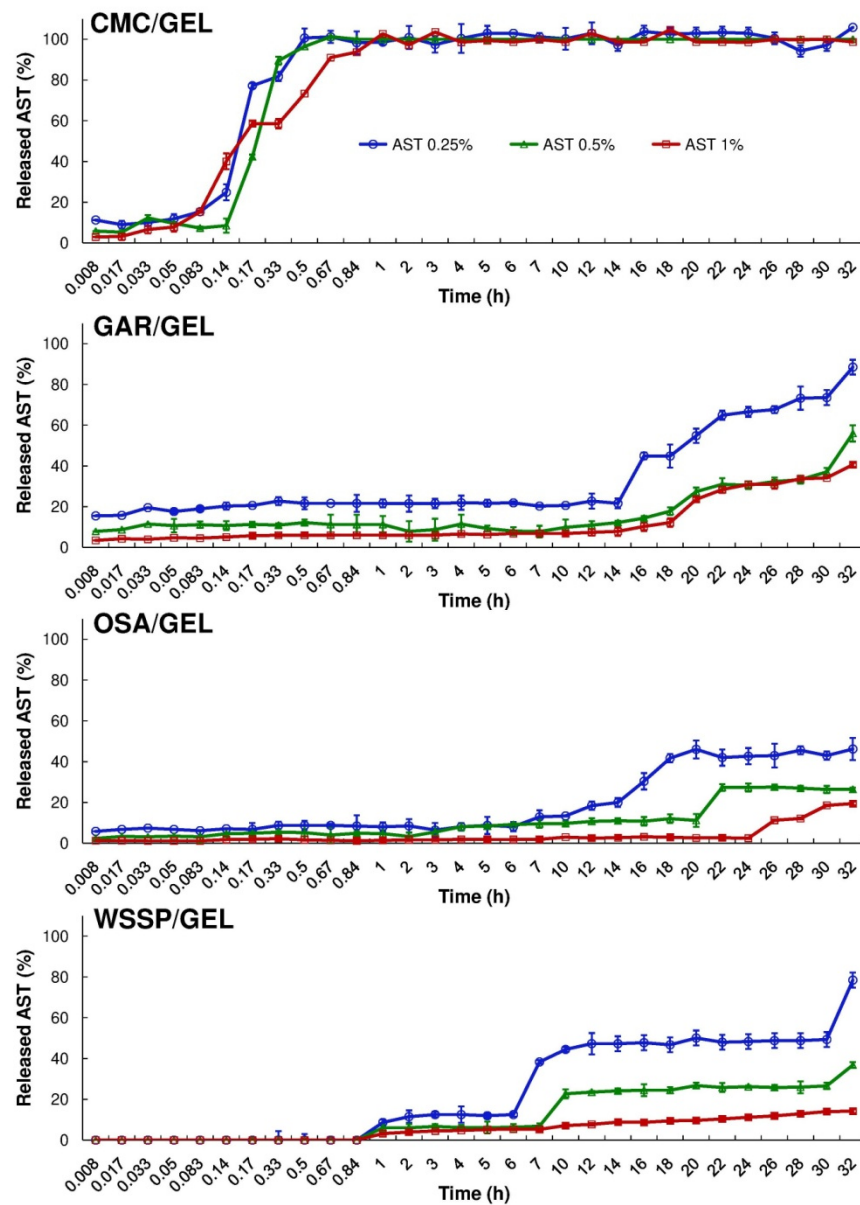


Figure 4. Percentage release of AST from the binary polysaccharide/GEL blend films into the water at 25 °C.

Table 3. Comparison of $R^2_{adjusted}$ values obtained from fitting experimental data to the different release models.

Film	AST (%)	Z-O T_{lag}	F-O F_{max}	Hig T_{lag}	Hop T_{lag}	K-P T_{lag}	Log 2	M-B T_{lag}	Wb F_{max}
CMC/GEL	0.25	0.2105	0.9503	0.2426	0.9575	0.9494	0.9606	0.7610	0.9610
	0.5	0.2194	0.9481	0.2567	0.9869	0.9410	0.9872	0.7517	0.9890
	1	0.2642	0.9824	0.3099	0.9824	0.9457	0.9821	0.9621	0.9829
GAR/GEL	0.25	0.8899	0.5867	0.7899	0.9238	0.9304	0.6389	0.9380	0.9180
	0.5	0.7780	0.5315	0.3689	0.9220	0.8642	0.5142	0.9341	0.7953
	1	0.8699	0.8289	0.7864	0.9231	0.8397	0.8397	0.9356	0.9106
OSA/GEL	0.25	0.9335	0.8729	0.8139	0.9314	0.9313	0.8736	0.9461	0.9287
	0.5	0.8852	0.7970	0.7472	0.8881	0.8906	0.8093	0.8861	0.7963
	1	0.5954	0.5911	0.8326	0.8446	0.8411	0.8404	0.8980	0.7422
WSSP/GEL	0.25	0.8523	0.9248	0.9192	0.8956	0.9162	0.9275	0.9187	0.9226
	0.5	0.8871	0.9412	0.9297	0.9037	0.9302	0.9439	0.9389	0.9425
	1	0.9281	0.9627	0.9832	0.9315	0.9827	0.9750	0.9967	0.9817
Average $R^2_{adjusted}$		0.6928	0.8265	0.6650	0.9242 *	0.9135	0.8577	0.9056	0.9059

* the best fit among the all models.

Table 4. Kinetic parameters obtained from two-parameter modeling.

Film	AST (%)	Z-O T_{lag}		F-O F_{max}		Hig T_{lag}	
		k_0	T_{lag}	k_1	F_{max}	k_H	T_{lag}
CMC/GEL	0.25	1.603	-41.703	4.399	101.594	17.865	-12.630
	0.5	1.740	-36.049	3.478	100.957	18.494	-9.997
	1	1.790	-34.293	3.230	99.919	18.721	-9.220
GAR/GEL	0.25	1.920	-8.124	0.008	355.699	11.542	-1.825
	0.5	0.959	-7.786	0.00009	15,279.747	6.265	1.758
	1	0.987	-3.007	0.00008	14,031.338	8.906	13.589
OSA/GEL	0.25	1.414	-4.041	0.027	85.433	8.259	1.882
	0.5	0.770	-4.465	0.013	85.507	4.555	1.783
	1	0.354	-1.155	0.00003	13,204.829	6.941	23.867
WSSP/GEL	0.25	2.077	-2.043	0.084	62.251	11.100	0.840
	0.5	1.077	-1.650	0.066	34.939	5.613	0.840
	1	0.443	-2.518	0.070	14.438	2.392	0.670

Table 5. Kinetic parameters obtained from three-parameter modeling.

Film	AST (%)	Hop T_{lag}			K-P T_{lag}			Log 2		
		k_{HB}	n	T_{lag}	k_{KP}	n	T_{lag}	α	β	F_{max}
CMC/GEL	0.25	2.224	1.433	-0.003	97.541	0.017	0.170	4.947	6.096	101.023
	0.5	2.805	0.421	-0.025	98.100	0.007	0.330	8.472	11.740	99.556
	1	0.009	371.689	0.008	86.585	0.055	0.140	2.552	3.563	100.352
GAR/GEL	0.25	0.021	0.525	-14.133	0.000	2.904	-45.281	-7.465	1.016	25,582.192
	0.5	0.017	0.160	-26.110	0.000	3.321	-44.884	-9.942	2.382	24,495.904
	1	0.023	0.222	-7.182	0.372	1.348	0.006	-10.486	3.112	13,213.903
OSA/GEL	0.25	0.012	1.243	-3.730	1.117	1.062	-4.771	-8.514	1.693	19,250.461
	0.5	0.017	0.336	-6.449	0.047	1.686	-13.899	-8.760	1.609	15,235.496
	1	0.026	0.051	-6.165	0.000	3.982	-0.068	-17.133	10.354	118.171
WSSP/GEL	0.25	0.000	212.634	-0.439	11.051	0.501	0.840	-3.559	4.060	60.547
	0.5	0.000	396.451	-0.901	4.454	0.577	0.696	-4.110	4.293	32.359
	1	0.000	122.841	-2.150	2.484	0.487	0.670	-3.876	1.489	83.440

Table 6. Kinetic parameters obtained from four-parameter modeling.

Film	AST (%)	M-B T_{lag}				Wb F_{max}				
		k_{MB}	n	k	T_{lag}	α	β	T_i	F_{max}	
CMC/GEL	0.25	82.488	0.234	0.023	0.008	0.057	2.112	-0.053	100.652	
	0.5	78.744	0.261	0.025	0.008	3.748	12.760	-0.858	99.641	
	1	89.040	0.097	0.008	0.140	0.321	0.858	0.027	99.944	
GAR/GEL	0.25	18.160	-0.058	-0.055	-0.775	17,018.112	2.012	-23.973	468.274	
	0.5	12.085	-0.442	-0.089	-1.822	1309.071	1.554	-14.722	153.488	
	1	4.794	0.009	-0.068	0.003	3059.906	1.849	-10.398	132.949	
OSA/GEL	0.25	0.001	3.757	0.066	-15.353	6993.898	1.065	-4.780	7756.062	
	0.5	0.128	1.393	-0.005	-11.203	110.319	0.722	0.027	255.772	
	1	0.600	-0.333	-0.147	-0.014	25,028.532	2.473	-4.127	63.672	
WSSP/GEL	0.25	6.969	0.819	0.023	0.622	21.504	1.409	0.001	54.429	
	0.5	1.575	1.197	0.038	0.013	38.243	1.561	-0.067	28.572	
	1	3.825	0.162	-0.025	0.840	98.199	0.495	0.670	243.555	

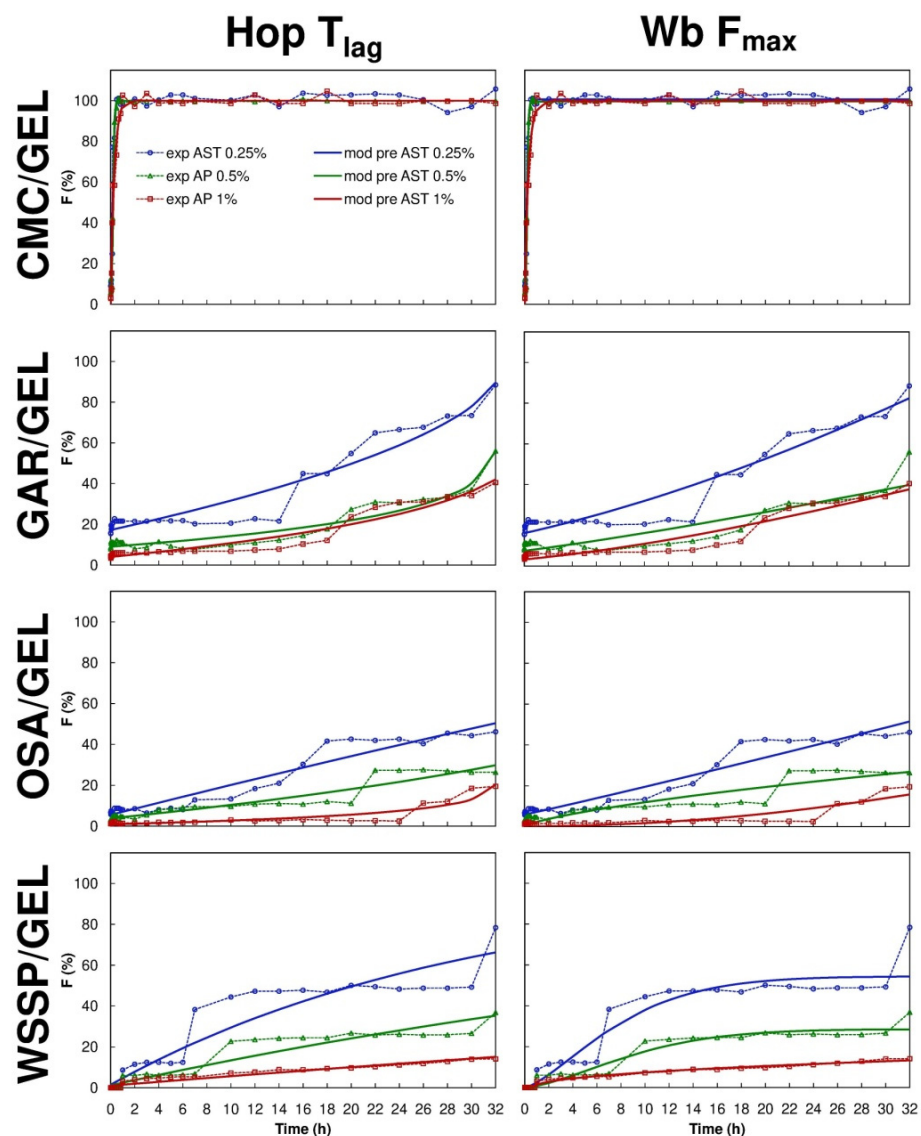


Figure 5. Fraction (F) of AST released from binary polysaccharide/GEL blend films according to the Hopfenberg with T_{lag} (*Hop* T_{lag}) and Weibull with F_{max} (*Wb* F_{max}) models; experimental (exp) and model predicted data (mod pre).

The $M-B$ T_{lag} model was the best to predict the release of AST from the GAR-based ($R^2_{adjusted} = 0.9341-0.9380$), OSA-based ($R^2_{adjusted} = 0.8861-0.9461$) and WSSP-based films ($R^2_{adjusted} = 0.9187-0.9967$). Interestingly, since the 1% AST-added WSSP/GEL film offered the most linear release profile (Figures 4 and 5), all mathematical models described fairly well the release from this system ($R^2_{adjusted} = 0.9281-0.9967$). The $K-P$ model is often used to analyse the release of the active substance from polymeric dosage forms, when the release mechanism is not well known, or when more than one type of release phenomena could be involved [30]. In planar (thin films) geometry, the released mechanism is described as: (i) quasi-Fickian diffusion ($n < 0.5$), (ii) Fickian diffusion ($n = 0.5$), (iii) non-Fickian diffusion ($0.5 < n < 1$), (iv) case II transport (zero-order release) ($n = 1$), and (v) super case II transport ($n > 1$) [31]. It was found that in the case of all CMC-based films, the n values were below 0.5 (Table 5), which implies that release mechanism was non-swellable matrix-diffusion [8,32]. It shows that the very small release exponent ($n = 0.007-0.055$) is characteristic for the burst release of AST (Figure 5). This result may be explained by the fact that despite the CMC/GEL film has short initial ability to hold water (swelling $\approx 500\%$), it rapidly dissolves (due to high content of easily soluble polysaccharide fraction) [8], which results

in a rapid dissolution of AST in the aqueous medium. This result supports evidence from previous observations [8], which showed that the release of potassium salts of iso- α -acids from the films based on CMC/GEL blends was beyond the limits of the K - P “power law” model ($n < 0.5$).

The release of AST from the 0.25–0.5% AST-added WSSP-based carrier and was followed by a non-Fickian mechanism. It shows that the AST migration was governed by diffusion and controlled swelling, whose rate was similar. The rearrangement of the polymeric chains occurred slowly, and the diffusion simultaneously caused the time-dependent anomalous release [33].

For the GAR- and OSA-based films (regardless of AST concentration), the n value was above 1, which is an indicator of the extreme form of transport (super case II model), i.e., more than one mechanism (swelling, polymer chain disentanglement (relaxation), erosion) was involved in the AST release kinetics. Regarding the GAR-based carrier, the obtained result complies with the previous findings [34,35], which suggested that gelling properties of GAR (at high polymer concentrations) ensure the sustained drug release. Thus, it can be concluded that the water entrapped in the gel strongly affected the diffusional behavior of AST in the GAR-based films. In turn, limited release of AST from the OSA/GEL carrier (~19–46%, depending on the AST concentration) could be attributed to the encapsulation of ASX in the OSA/GEL complexes (coacervates) [36].

As for the 1% AST-added WSSP-based film, it is possible that the bulky amounts of starch granules (from AST) acted as a release modifier. It is known that native starch has multifunctional uses in the different physical forms of carriers serving as the binder, disintegrant, diluents, glidant, and lubricant [37]. Therefore, it is possible that the granules anchored in the film matrix (Figure 1), hindered the contact of dissolution media with WSSP/GEL matrix, which consequently limited erosion of the carrier, thus ASX release was predominately controlled by diffusion ($n < 0.5$, Table 5).

4. Conclusions

The CMC-based carrier offers a quasi-Fickian release of AST with the burst effect (100% release occurred after 0.5–1 h, depending on the AST concentration). According to the $t_{25\%}$, at the lowest AST concentration (0.25%), the OSA/GEL film offered about 1.9, 2.2, and 148.2 times slower release compared to the GAR-, WSSP- and CMC-based carriers, respectively. The 1% AST-added WSSP-based system had the most linear AST release profile (close to the Z - O kinetics). It suggests that this formulation applied on the high moisture food will maintain the main dose of the carotenoid on the surface, where the oxidation reactions occur the most intensively. It was found that the Hopfenberg with T_{lag} model provided the best fit for all release series data. The Korsmeyer–Peppas release exponent (n), for the GAR-, OSA-, and WSSP-based films was >0.5 , confirming that these carriers ensured more multi-mechanistic AST release than the CMC-based film ($n < 0.5$).

In summary, this study showed that apart from the CMC/GEL carrier, the migration of AST from the films into the water at 25 °C (the highest predictable food/packaging contact temperature) was incomplete, although the compound was released for more than one day. The release tests were limited only to 32 h because of a further progressive spoilage of film samples (the presence of a bad odour coming from the acceptor solution). Therefore, the accelerated release testing at increased temperature (e.g., 30 °C) can be recommended to rapidly assess and predict “real-time” AST release profiles from the obtained films.

In order to facilitate the selection of suitable candidate material for a particular packaging application, further experimental investigations are needed to estimate the effect of increasing concentration of AST on the optical, mechanical, and barrier properties of the binary polysaccharide/GEL blend films.

Author Contributions: Conceptualization, K.Ł. and D.K.; methodology, D.K.; validation, K.Ł. and D.K.; formal analysis, K.Ł.; investigation, K.Ł. and T.S.; data curation, K.Ł.; writing—original draft preparation, K.Ł.; writing—review and editing, D.K. and B.B.; visualization, K.Ł.; supervision, D.K. and B.B.; project administration, K.Ł.; funding acquisition, K.Ł. All authors have read and agreed to the published version of the manuscript.

Funding: This work was financially supported by the National Science Centre (Poland) under grant number 2019/35/N/NZ9/01795.

Data Availability Statement: The data present in this study are available on request from the first author (Katarzyna Łupina).

Conflicts of Interest: The authors declare no conflict of interest.

References

1. Nyamweya, N.N. Applications of polymer blends in drug delivery. *Future J. Pharm. Sci.* **2021**, *7*, 18. [[CrossRef](#)]
2. Cutter, C.N. Microbial control by packaging: A review. *Crit. Rev. Food Sci. Nutr.* **2002**, *42*, 151–161. [[CrossRef](#)] [[PubMed](#)]
3. Kowalczyk, D. Biopolymer/candelilla wax emulsion films as carriers of ascorbic acid—A comparative study. *Food Hydrocoll.* **2016**, *52*, 543–553. [[CrossRef](#)]
4. Kowalczyk, D.; Biendl, M. Physicochemical and antioxidant properties of biopolymer/candelilla wax emulsion films containing hop extract—A comparative study. *Food Hydrocoll.* **2016**, *60*, 384–392. [[CrossRef](#)]
5. Young, S.; Wong, M.; Tabata, Y.; Mikos, A.G. Gelatin as a delivery vehicle for the controlled release of bioactive molecules. *J. Control. Release* **2005**, *109*, 256–274. [[CrossRef](#)] [[PubMed](#)]
6. Uz, M.; Altinkaya, S.A. Development of mono and multilayer antimicrobial food packaging materials for controlled release of potassium sorbate. *LWT—Food Sci. Technol.* **2011**, *44*, 2302–2309. [[CrossRef](#)]
7. Łupina, K.; Kowalczyk, D.; Zięba, E.; Kazimierczak, W.; Meżyńska, M.; Basiura-Cembala, M.; Wiącek, A.E. Edible films made from blends of gelatin and polysaccharide-based emulsifiers—A comparative study. *Food Hydrocoll.* **2019**, *96*, 555–567. [[CrossRef](#)]
8. Kowalczyk, D.; Pytka, M.; Szymanowska, U.; Skrzypek, T.; Łupina, K.; Biendl, M. Release kinetics and antibacterial activity of potassium salts of iso- α -acids loaded into the films based on gelatin, carboxymethyl cellulose and their blends. *Food Hydrocoll.* **2020**, *109*, 106104. [[CrossRef](#)]
9. Kowalczyk, D.; Kordowska-Wiater, M.; Karaś, M.; Zięba, E.; Meżyńska, M.; Wiącek, A.E. Release kinetics and antimicrobial properties of the potassium sorbate-loaded edible films made from pullulan, gelatin and their blends. *Food Hydrocoll.* **2020**, *101*, 105539. [[CrossRef](#)]
10. Kowalczyk, D.; Baraniak, B. Effect of candelilla wax on functional properties of biopolymer emulsion films—A comparative study. *Food Hydrocoll.* **2014**, *41*, 195–209. [[CrossRef](#)]
11. Chiwele, I.; Jones, B.E.; Podczec, F. The shell dissolution of various empty hard capsules. *Chem. Pharm. Bull.* **2000**, *48*, 951–956. [[CrossRef](#)]
12. Liu, C.; Huang, J.; Zheng, X.; Liu, S.; Lu, K.; Tang, K.; Liu, J. Heat sealable soluble soybean polysaccharide/gelatin blend edible films for food packaging applications. *Food Packag. Shelf Life* **2020**, *24*, 100485. [[CrossRef](#)]
13. Jridi, M.; Abdelhedi, O.; Salem, A.; Kechaou, H.; Nasri, M.; Menchari, Y. Physicochemical, antioxidant and antibacterial properties of fish gelatin-based edible films enriched with orange peel pectin: Wrapping application. *Food Hydrocoll.* **2020**, *103*, 105688. [[CrossRef](#)]
14. Kowalczyk, D.; Szymanowska, U.; Skrzypek, T.; Basiura-Cembala, M.; Łupina, K.; Biendl, M. Edible films based on gelatin, carboxymethyl cellulose, and their blends as carriers of potassium salts of iso- α -acids: Structural, physicochemical and antioxidant properties. *Food Hydrocoll.* **2021**, *115*. [[CrossRef](#)]
15. Kowalczyk, D.; Skrzypek, T.; Basiura-Cembala, M.; Łupina, K.; Meżyńska, M. The effect of potassium sorbate on the physicochemical properties of edible films based on pullulan, gelatin and their blends. *Food Hydrocoll.* **2020**, *105*, 105837. [[CrossRef](#)]
16. Łupina, K.; Kowalczyk, D.; Drożdowska, E. Polysaccharide/gelatin blend films as carriers of ascorbyl palmitate—A comparative study. *Food Chem.* **2020**, *333*, 127465. [[CrossRef](#)]
17. Łupina, K.; Kowalczyk, D.; Kazimierczak, W. Gum Arabic/gelatin and water-soluble soy polysaccharides/gelatin blend films as carriers of astaxanthin—A comparative study of the kinetics of release and antioxidant properties. *Polymers* **2021**, *13*, 1062. [[CrossRef](#)]
18. Fakhri, S.; Abbaszadeh, F.; Dargahi, L.; Jorjani, M. Astaxanthin: A mechanistic review on its biological activities and health benefits. *Pharmacol. Res.* **2018**, *136*, 1–20. [[CrossRef](#)] [[PubMed](#)]
19. Yamashita, E. Astaxanthin as a Medical Food. *Funct. Foods Health Dis.* **2013**, *3*, 254–258. [[CrossRef](#)]
20. Landon, R.; Gueguen, V.; Petite, H.; Letourneur, D.; Pavon-Djavid, G.; Anagnostou, F. Impact of Astaxanthin on Diabetes Pathogenesis and Chronic Complications. *Mar. Drugs* **2020**, *18*, 357. [[CrossRef](#)] [[PubMed](#)]
21. Donoso, A.; González-Durán, J.; Muñoz, A.A.; González, P.A.; Agurto-Muñoz, C. Therapeutic uses of natural astaxanthin: An evidence-based review focused on human clinical trials. *Pharmacol. Res.* **2021**, *166*. [[CrossRef](#)]

22. Faraone, I.; Sinisgalli, C.; Ostuni, A.; Armentano, M.F.; Carmosino, M.; Milella, L.; Russo, D.; Labanca, F.; Khan, H. Astaxanthin anticancer effects are mediated through multiple molecular mechanisms: A systematic review. *Pharmacol. Res.* **2020**, *155*, 104689. [[CrossRef](#)]
23. Brendler, T.; Williamson, E.M. Astaxanthin: How much is too much? A safety review. *Phyther. Res.* **2019**, *33*, 3090–3111. [[CrossRef](#)] [[PubMed](#)]
24. Capelli, B.; Bagchi, D.; Cysewski, G.R. Synthetic astaxanthin is significantly inferior to algal-based astaxanthin as an antioxidant and may not be suitable as a human nutraceutical supplement. *Nutraceuticals* **2013**, *12*, 145–152. [[CrossRef](#)]
25. Koller, M.; Muhr, A.; Braunegg, G. Microalgae as versatile cellular factories for valued products. *Algal Res.* **2014**, *6*, 52–63. [[CrossRef](#)]
26. Colín-Chávez, C.; Soto-Valdez, H.; Peralta, E.; Lizardi-Mendoza, J.; Balandrán-Quintana, R. Diffusion of natural astaxanthin from polyethylene active packaging films into a fatty food simulant. *Food Res. Int.* **2013**, *54*, 873–880. [[CrossRef](#)]
27. Zhang, Y.; Huo, M.; Zhou, J.; Zou, A.; Li, W.; Yao, C.; Xie, S. DDSolver: An add-in program for modeling and comparison of drug dissolution profiles. *AAPS J.* **2010**, *12*, 263–271. [[CrossRef](#)]
28. Singh, J.; Colussi, R.; McCarthy, O.J.; Kaur, L. Potato Starch and Its Modification. In *Advances in Potato Chemistry and Technology*, 2nd ed.; Singh, J., Kaur, L., Eds.; Elsevier Inc.: Amsterdam, The Netherlands, 2016; pp. 195–247. ISBN 9780128000021. Available online: <https://www.sciencedirect.com/science/article/pii/B978012800002100008X> (accessed on 1 February 2021).
29. Ikeda, S.; Funami, T.; Zhang, G. Visualizing surface active hydrocolloids by atomic force microscopy. *Carbohydr. Polym.* **2005**, *62*, 192–196. [[CrossRef](#)]
30. Costa, P.; Lobo, J.M.S. Modeling and comparison of dissolution profiles. *Eur. J. Pharm. Sci.* **2001**, *13*, 123–133. [[CrossRef](#)]
31. Olejnik, A.; Kapuscinska, A.; Schroeder, G.; Nowak, I. Physico-chemical characterization of formulations containing endomorphin-2 derivatives. *Amino Acids* **2017**, *49*, 1719–1731. [[CrossRef](#)]
32. Permanadewi, I.; Kumoro, A.C.; Wardhani, D.H.; Aryanti, N. Modelling of controlled drug release in gastrointestinal tract simulation. *J. Phys. Conf. Ser.* **2019**, *1295*, 012063. [[CrossRef](#)]
33. Bruschi, M. Mathematical models of drug release. In *Strategies to Modify the Drug Release from Pharmaceutical Systems*; Bruschi, M., Ed.; Woodhead Publishing: Cambridge, UK, 2015; pp. 63–86. ISBN 9780081000922.
34. Shah, S.N.H.; Asghar, S.; Choudhry, M.A.; Akash, M.S.H.; Rehman, N.U.; Baksh, S. Formulation and evaluation of natural gum-based sustained release matrix tablets of flurbiprofen using response surface methodology. *Drug Dev. Ind. Pharm.* **2009**, *35*, 1470–1478. [[CrossRef](#)]
35. Batra, V.; Bhowmick, A.; Behera, B.K.; Ray, A.R. Sustained release of ferrous sulfate from polymer-coated gum arabica pellets. *J. Pharm. Sci.* **1994**, *83*, 632–635. [[CrossRef](#)] [[PubMed](#)]
36. Zhao, Y.; Khalid, N.; Shu, G.; Neves, M.A.; Kobayashi, I.; Nakajima, M. Complex coacervates from gelatin and octenyl succinic anhydride modified kudzu starch: Insights of formulation and characterization. *Food Hydrocoll.* **2019**, *86*, 70–77. [[CrossRef](#)]
37. Builders, P.F.; Arhewoh, M.I. Pharmaceutical applications of native starch in conventional drug delivery. *Starch/Stärke* **2016**, *68*. [[CrossRef](#)]